

Calculation on Fluctuation of Water Surface in Ship Lift Chamber under Water Level Difference

Xiaomeng Cao^{1*}, Zhenghua Gu²

¹College of Engineering, Zhejiang Open University, Hangzhou, China

²College of Civil Engineering and Architecture, Zhejiang University, Hangzhou, China

Email: *11112010@zju.edu.cn

How to cite this paper: Cao, X.M. and Gu, Z.H. (2025) Calculation on Fluctuation of Water Surface in Ship Lift Chamber under Water Level Difference. *Journal of Applied Mathematics and Physics*, 13, 429-444.
<https://doi.org/10.4236/jamp.2025.132022>

Received: January 10, 2025

Accepted: February 14, 2025

Published: February 17, 2025

Copyright © 2025 by author(s) and Scientific Research Publishing Inc. This work is licensed under the Creative Commons Attribution International License (CC BY 4.0).

<http://creativecommons.org/licenses/by/4.0/>



Open Access

Abstract

Upon ship lift chamber docking with approach channel in the case of water level difference, water in chamber will fluctuate evidently. The maximum or minimum fluctuation of water surface is an important parameter to measure operational safety of ship lift. A simplified 3D mathematical model of ship lift chamber upon tumble gate opening was built based on standard $k-\varepsilon$ model, FVM (Finite Volume Method) and VOF (Volume of Fluid) model. Based on π theorem, the dimensionless influencing factors of $\Delta h_{\max}/d$ and $\Delta h_{\min}/d$ were B/L , d/B and $\Delta h/d$. On this basis, 30 sets of working conditions were designed to respectively study the relationships between the maximum wave height and each influencing factor. Through regression analysis, the empirical formulas of $\Delta h_{\max}/d$ and $\Delta h_{\min}/d$ were obtained. Furthermore, taking into account the potential influence of the gate opening time on the wave height in practical applications, the relationship between the gate opening time and the error was fitted, and the modified empirical formulas of $\Delta h'_{\max}/d$ and $\Delta h'_{\min}/d$ were derived, which had a wider scope of application. The results have practical value for engineering design and security operation of ship lift.

Keywords

Ship Lift, Chamber, Water Wave, VOF Model, FVM, CFD

1. Introduction

Ship lift is a common navigation structure, which uses mechanical power to drag the lock chamber to move up and down, so as to overcome the drop of concentrated water level in the waterway. Compared with the ship lock, the ship lift has

the advantages of less water consumption, fast running speed, small lifting height limited by technical conditions, and lower investment speed of using water head than the ship lock [1]. It is hailed as the “elevator for ships” and is widely applied in navigation of high dams [2]. Since the 1780s, the research and application of ship lifts have been started. China, Britain, Germany, Belgium, France and other countries have rich experience in building medium and large ship lifts [3]. At present, the largest ship lift in the world is a three-stage vertical ship lift located in Goupitan, Wujiang, Guizhou, China, with a total lifting height of 199 m, among which the lifting height of the intermediate ship lift is as high as 127 m [1].

The operation process of ship lift can be summarized into three steps: ship entry, lifting and lowering, and ship exit. Among them, the aerial lifting and lowering stage usually has a simple process and runs smoothly, while the stages of caisson docking and ships entering and leaving the caisson are more complicated, with numerous influencing factors [4] [5]. If the water level changes too fast or the amplitude is too large, it will prolong the docking time, increase the docking difficulty and even make it impossible to dock [6]. During the docking of the chamber with the upper and lower lock heads, the water depth in the chamber will change with the fluctuations of the water levels in the upstream and downstream waterways. Excessive changes in water depth may cause ships to touch the bottom, water to overflow from the caisson, ships to lose control, longitudinal instability [7], and may even lead to accidents. In Germany, there was once an accident where a small ship caisson capsized [8]. Therefore, the hydrodynamic issues of the ship lift caisson when the gates are opened and closed are highly worthy of attention, as they are the prerequisite for ensuring the practicability and risk-free operation of the ship lift.

In this regard, Chinese researchers have conducted more investigations and studies [3] [9]-[13]. Relying on various projects within China and based on theoretical analyses as well as the results of a series of model tests of multiple ship lifts, they have solved the hydrodynamic safety problems such as ships entering and leaving the caisson, the opening and closing of the caisson doors, and caisson docking. This has provided a scientific basis for formulating the operating regulations and industry standards for ship lifts [1]. Compared with Chinese scholars, researchers from other countries are more inclined to adopt numerical simulation methods. They extended the study of the water flow problem in the ship lift chamber during the opening or closing of the flap gate to the flow characteristics of the variable area, or the wave or sloshing problems in shallow and narrow water areas [14]-[19], and three-dimensional variable regions through self-developed programs or existing models [20] [21]. The solution of boundary integral equation and the treatment method of dynamic grid can provide a reference for the hydrodynamic problems of ship lift chamber when flap gate is opened and closed.

During the actual operation of the ship lift, there is usually a water level difference when the ship lift chamber is docked with the approach channel. Especially when docking with the downstream approach channel, which has a large water level amplitude and a rapid change rate, the water level difference will be greater

and more difficult to control [3]. Under such circumstances, when the caisson door of the ship lift is opened or closed, the water in the caisson is squeezed by the door, and due to the existence of the water level difference inside and outside the caisson, the water surface in the caisson fluctuates. This not only affects the berthing safety of ships in the caisson, but also impacts the overall operational safety of the ship lift [1]. The maximum or minimum water surface fluctuation is one of the important parameters that serves as a crucial indicator for measuring the critical instability water depth, the designed water depth of the caisson, the maximum allowable water level difference, and the ship berthing conditions. In this study, a simplified three-dimensional mathematical model of the ship lift chamber during the opening of the flap gate was established based on the standard $k-\varepsilon$ model, the Finite Volume Method (FVM), and the Volume of Fluid (VOF) model. The impacts of the geometric dimensions of the ship caisson and the water level difference inside and outside the caisson on the wave fluctuation characteristics were also discussed.

2. Mathematical Model

2.1. Governing Equations

The hydrodynamic problem on tumble gate opening is exhibited in **Figure 1**. In order to facilitate simulation, the case of no ship in chamber is considered and the gate opening process is simplified as removing the gate suddenly (**Figure 1**). The simplified flow problem is generalized in **Figure 2**. The smooth transition region between chamber and approach channel is to prevent wave reflection from sudden expansion section. The water level difference between approach channel and chamber is Δh . And when the water level in approach channel is higher than chamber, Δh is defined as positive, otherwise, negative. X direction is along chamber length, Y is along water depth and Z is along chamber width. Under above Cartesian coordinate system, the governing equations of standard $k-\varepsilon$ model of incompressible, viscous, homogeneous fluid flow can be expressed as follows.

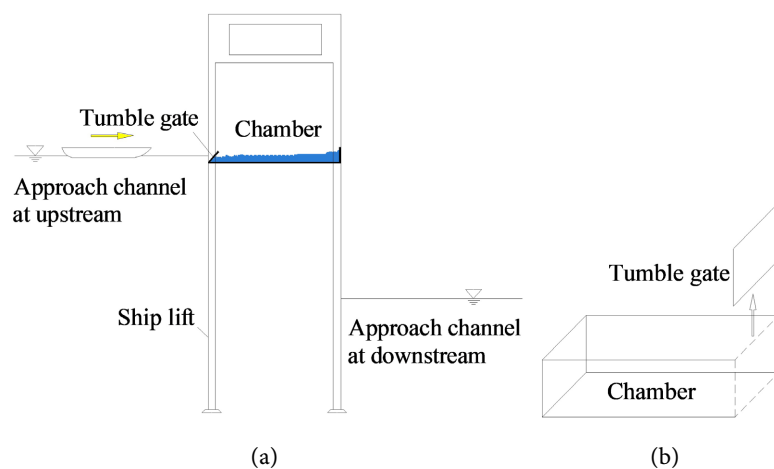


Figure 1. Hydrodynamic problem on tumble gate opening (a), simplified gate opening (b).

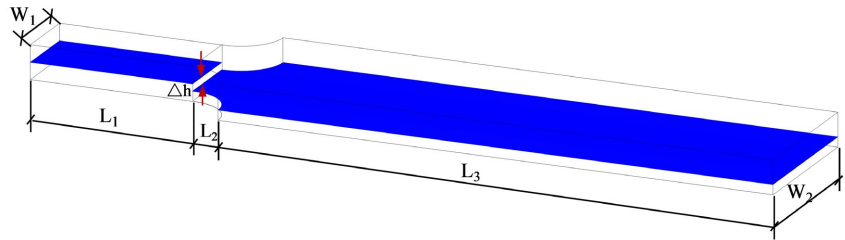


Figure 2. Simplified flow model.

Continuity equation

$$\frac{\partial U_i}{\partial X_i} = 0 \tag{1}$$

Motion equation

$$\frac{\partial U_i}{\partial t} + \frac{\partial}{\partial X_j} (U_i U_j) = -\frac{1}{\rho} \frac{\partial p}{\partial X_i} + \frac{\partial}{\partial X_j} \left[\left(\nu + \nu_t \right) \left(\frac{\partial U_i}{\partial X_j} + \frac{\partial U_j}{\partial X_i} \right) \right] \tag{2}$$

Turbulent kinetic energy equation

$$\frac{\partial k}{\partial t} + U_i \frac{\partial k}{\partial X_i} = \frac{\partial}{\partial X_i} \left[\left(\nu + \frac{\nu_t}{\sigma_k} \right) \frac{\partial k}{\partial X_i} \right] + G - \varepsilon \tag{3}$$

Turbulent dissipation rate equation

$$\frac{\partial \varepsilon}{\partial t} + U_i \frac{\partial \varepsilon}{\partial X_i} = \frac{\partial}{\partial X_i} \left[\left(\nu + \frac{\nu_t}{\sigma_\varepsilon} \right) \frac{\partial \varepsilon}{\partial X_i} \right] + C_{1\varepsilon} \frac{\varepsilon}{k} G - C_{2\varepsilon} \frac{\varepsilon^2}{k} \tag{4}$$

where U_i is the velocity in three directions; ρ is the fluid density; t is the time; p is the pressure; ν is the kinematic viscosity coefficient; ν_t is the turbulence viscosity

coefficient, $\nu_t = \rho C_\mu k^2 / \varepsilon$; G is the production term, $G = \nu_t \left(\frac{\partial U_i}{\partial X_j} + \frac{\partial U_j}{\partial X_i} \right) \frac{\partial U_i}{\partial X_j}$.

The empirical constants in Equations (3) and (4) are as follows: $C_{1\varepsilon} = 1.44$, $C_{2\varepsilon} = 1.92$, $\sigma_k = 1.0$, $\sigma_\varepsilon = 1.3$, $C_\mu = 0.09$.

2.2. Materials

2.2.1. CFD Tool and Meshes

The commercial CFD software code—FLUENT is chosen to fulfill the relevant simulation. Based on the dimensions in Reference [6], geometric model is established by GAMBIT. Since the simulation area is regular, hexahedral structured meshes are adopted and refined in chamber area. And the local meshes are shown in **Figure 3**. To define the model, pressure-based solver and standard k - ε model are selected. To solve, the coupling of pressure-velocity utilizes PISO (Pressure Implicit with Splitting of Operators), pressure discretization utilizes PRESTO and the discrete format of momentum. For boundary conditions, vertical planes and flume bottom are regarded as wall and meet no-slip condition. VOF (Volume of Fluid) model is utilized for water face simulation. Volume function of one fluid (water or air) in control volume is $F(x, y, z, t)$, $F \in [0, 1]$, and the transport equation is expressed as:

$$\frac{\partial F}{\partial t} + u_i \nabla F = 0 \quad (5)$$

In VOF model, volume fraction α_q is introduced. And $\alpha_q = 0$ represents there is no q -phase fluid in control grid, $\alpha_q = 1$ represents the control volume is full of q -phase fluid and $0 < \alpha_q < 1$ indicates the grid contains interface between fluids. The sum of volume fraction in each control grid is 1. Accordingly, flume top is set as pressure-in. The outlet is far from chamber to ensure flow full development and the corresponding boundary is set as wall.

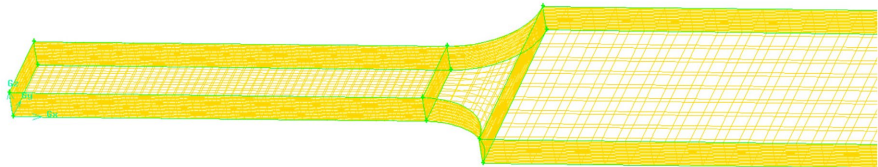


Figure 3. Local meshes scheme.

2.2.2. Model Verification

To verify the accuracy of mathematical models, two sets of verification conditions listed in **Table 1** are conducted firstly. The water level in chamber is d and in approach is d_1 . L_3 is ten times of $(L + L_2)$ to avoid the impact from approach channel. Three measure points identified in **Figure 4** are arranged at the bottom of flume along the inner wall of the ship-lift chamber.

Table 1. Verification conditions.

No.	d (cm)	d_1 (cm)	Δh (cm)	L (m)	L_2 (m)	L_3 (m)	B (m)	B_1 (m)	H (m)
v1	14	18	4	4.67	0.86	55.3	1.08	2.8	0.3
v2	14	10	-4						

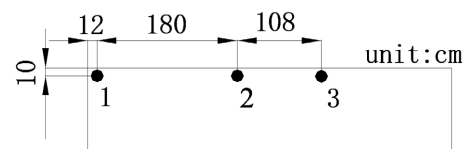


Figure 4. Monitoring points.

When the water level in the approach channel is higher than the water level in chamber, we call it “forward water level difference”, and at this time, Δh is positive. On the other hand, when the water level in the approach channel is lower than the water level in the chamber, we call it “reverse water level difference”, and Δh is negative. Under forward water level difference, the water fluctuation in chamber hardly fall below the initial surface; while under reverse water level difference, the water fluctuation in chamber hardly high than initial surface [6]. Therefore, we only study the maximum wave height under forward water level difference and the minimum wave height under reverse water level difference respectively. **Figure 5** shows the definition of maximum wave height Δh_{\max} and minimum wave

height Δh_{\min} . **Figure 6** exhibits the comparison of Δh_{\max} of v1 and Δh_{\min} of v2 between observed results from experiments and computed results from mathematical model at the three monitoring points. Noted that the observed data in this paper are from Reference [6]. The simulation results are reasonably consistent with those of the experimental measurements. The errors between the two may be attributed to the different opening ways of tumble gate.

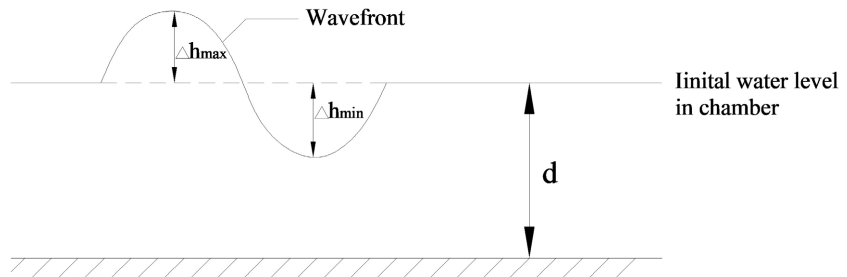


Figure 5. Definition of wave height.

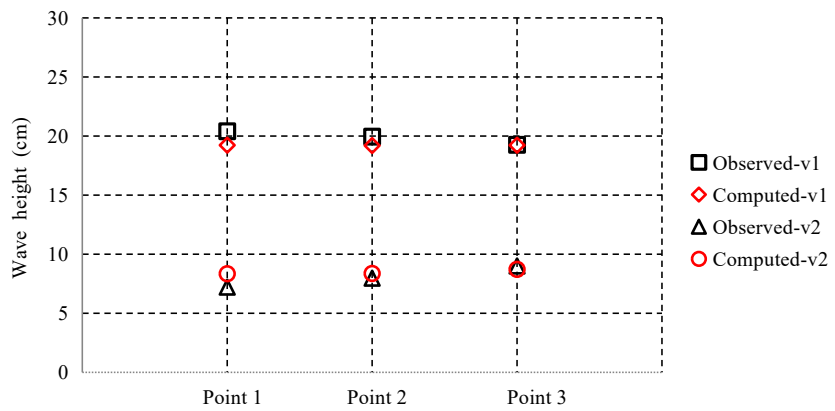


Figure 6. Comparison between observed and computed under v1 and v2.

Further measure the stage hydrograph of monitoring point 1 under the verification conditions. **Figure 7** and **Figure 8** show the comparison of stage hydrograph between numerical simulation and model test. Observe that the computed results are in good agreement with the observed results in the period, but there are some deviations in the maximum rising height of water waves and the attenuation envelope of water waves.

The main reasons for the deviation are concentrated in the following aspects. First of all, compared to suddenly removing the gate, the open way of flipping the gate in physical experiment will aggravate the disturbance of the water in the ship lift chamber, so that the maximum rising height of water waves in the physical model experiment is slightly larger than that in the mathematical model experiment. Secondly, in the physical experiment, the water surface fluctuation was measured by capacitance water-level gauge, and the water surface fluctuation period was measured by stopwatch. The experimental results of water surface fluctuation are greatly influenced by the sampling interval time, especially when the water surface changes violently in the chamber, which is one of the reasons why the error between the

two (physical and mathematical models) is relatively large when the amplitude of water-surface fluctuations is large. Thirdly, the design of the physical model experiment was based on the Yantan Ship Lift in Guangxi Province, China. To verify the rationality of the physical experiment design, the experimental results were compared with those of another physical model experiment (control experiment) that had been accepted and applied by the design and construction units. The results of the two experiments were similar, with a small error. In the physical model experiment of this paper, in order to reduce the reflection of water waves by the downstream wall, a certain amount of stones were laid downstream in the flume to dissipate waves and energy. The layout of this series of measures was also based on the control experiment, and the results were verified. However, in numerical simulations, it is difficult to accurately measure the magnitude of this wave elimination effect, thus leading to deviations in the envelope line. Apart from the reasons mentioned above, there are some other uncertainties in the physical experiments. But on the whole, the comparison results show that our numerical model is convincing.

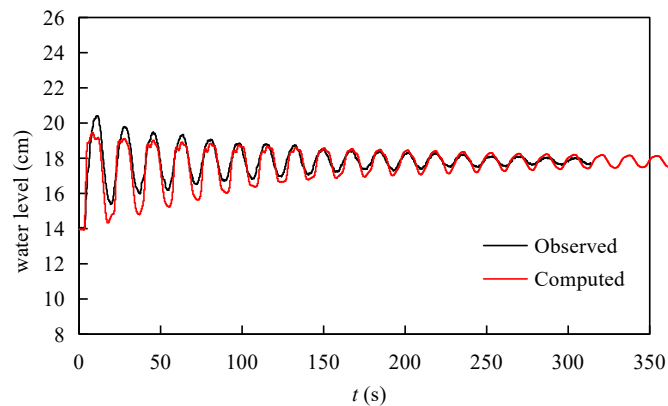


Figure 7. Comparison of stage hydrograph between observed and computed under v1.

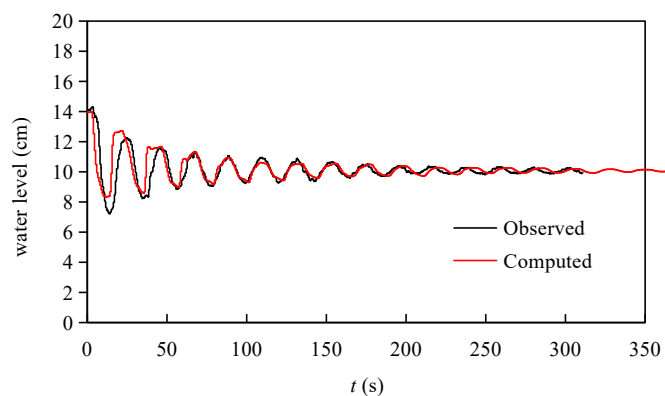


Figure 8. Comparison of stage hydrograph between observed and computed under v2.

2.2.3. Dimensional Analysis and Conditions

In the case of non-ship and simplified opening way of tumble gate, the main influencing factors of chamber hydrodynamic characteristics include two categories.

First is geometry, including chamber length L , chamber width B , initial water level in chamber d and initial water level difference Δh ; second is dynamics, including water density ρ and gravitational acceleration g . The function expression can be written as follows:

$$y = f(L, B, \Delta h, d, \rho, g) \quad (6)$$

where y represents chamber hydrodynamic characteristics, and here is maximum wave height Δh_{\max} or minimum wave height Δh_{\min} . According to π theorem, ρ , g and d are selected as basic variables, and dimensionless equations are obtained as Equation (7).

$$\begin{cases} \frac{\Delta h_{\max}}{d} = f\left(\frac{B}{L}, \frac{d}{B}, \frac{\Delta h}{d}\right) \\ \frac{\Delta h_{\min}}{d} = f\left(\frac{B}{L}, \frac{d}{B}, \frac{\Delta h}{d}\right) \end{cases} \quad (7)$$

where B/L is chamber width to length, which is used to measure the chamber longitudinal stability; d/B is water depth to chamber width; $\Delta h/d$ is relative level difference. On the basis of Equation (7), 30 sets of conditions which are listed in **Table 2** are draw up for further research on the variation of Δh_{\max} or Δh_{\min} with every influencing factor.

Table 2. Simulation conditions.

No.	L (m)	B (m)	d (m)	Δh (m)	d/B	B/L	$\Delta h/d$
1	4.67	1.08	0.14	0.01	0.13	0.231	0.071
2	4.67	1.08	0.14	0.02	0.13	0.231	0.143
3	4.67	1.08	0.14	0.03	0.13	0.231	0.214
4	4.67	1.08	0.14	0.04	0.13	0.231	0.286
5	4.67	1.08	0.14	0.05	0.13	0.231	0.357
6	4.67	1.08	0.14	-0.01	0.13	0.231	-0.071
7	4.67	1.08	0.14	-0.02	0.13	0.231	-0.143
8	4.67	1.08	0.14	-0.03	0.13	0.231	-0.214
9	4.67	1.08	0.14	-0.04	0.13	0.231	-0.286
10	4.67	1.08	0.14	-0.05	0.13	0.231	-0.357
11	2.50	1.08	0.14	0.04	0.13	0.432	0.286
12	3.50	1.08	0.14	0.04	0.13	0.309	0.286
13	4.67	1.08	0.14	0.04	0.13	0.231	0.286
14	5.50	1.08	0.14	0.04	0.13	0.196	0.286
15	6.50	1.08	0.14	0.04	0.13	0.166	0.286
16	2.50	1.08	0.14	-0.04	0.13	0.432	-0.286
17	3.50	1.08	0.14	-0.04	0.13	0.309	-0.286
18	4.67	1.08	0.14	-0.04	0.13	0.231	-0.286
19	5.50	1.08	0.14	-0.04	0.13	0.196	-0.286

Continued

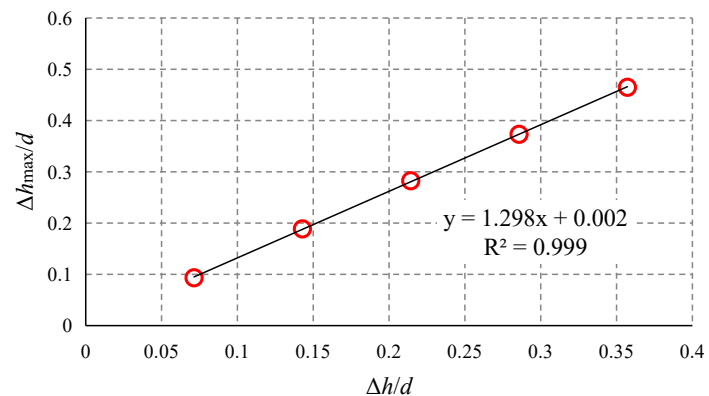
20	6.50	1.08	0.14	-0.04	0.13	0.166	-0.286
21	4.67	1.08	0.08	0.023	0.074	0.231	0.286
22	4.67	1.08	0.10	0.029	0.093	0.231	0.286
23	4.67	1.08	0.13	0.037	0.120	0.231	0.286
24	4.67	1.08	0.14	0.040	0.130	0.231	0.286
25	4.67	1.08	0.15	0.043	0.139	0.231	0.286
26	4.67	1.08	0.08	-0.023	0.074	0.231	-0.286
27	4.67	1.08	0.10	-0.029	0.093	0.231	-0.286
28	4.67	1.08	0.13	-0.037	0.120	0.231	-0.286
29	4.67	1.08	0.14	-0.040	0.130	0.231	-0.286
30	4.67	1.08	0.15	-0.043	0.139	0.231	-0.286

Note: No. 4, 13 and 24 are same; No. 9, 18 and 29 are same.

3. Results and Discussion

3.1. Variable Influence Law

According to experimental results in Reference [6], the position of maximum and minimum wave height is often near the fixed vertical wall of chamber, so Point 1 (identified in Figure 4) is selected as study point in the following. Figure 9 exhibits the profile of $\Delta h_{\max}/d$ and $\Delta h_{\min}/d$ with $\Delta h/d$ at Point 1 respectively. It is very evident that the relationship between the two coordinate axes is linear either under positive or negative water level difference. As absolute value of water level difference increases, absolute value of $\Delta h_{\max}/d$ or $\Delta h_{\min}/d$ increases, which shows after removing the tumble gate the larger the water level difference, the harder the fluctuation. In addition, the slopes of lines in Figure 9(a) and Figure 9(b) are almost equal, that is, the average change rate of $\Delta h_{\max}/d$ and $\Delta h_{\min}/d$ with $\Delta h/d$ is general equal. Further compared the data of Figure 9(a) and Figure 9(b), it can be found that when the absolute values of water level difference are equal, the absolute values of $\Delta h_{\min}/d$ and $\Delta h_{\max}/d$ are almost equal too, which implies when water level difference is equal but opposite, waveforms are symmetry.



(a)

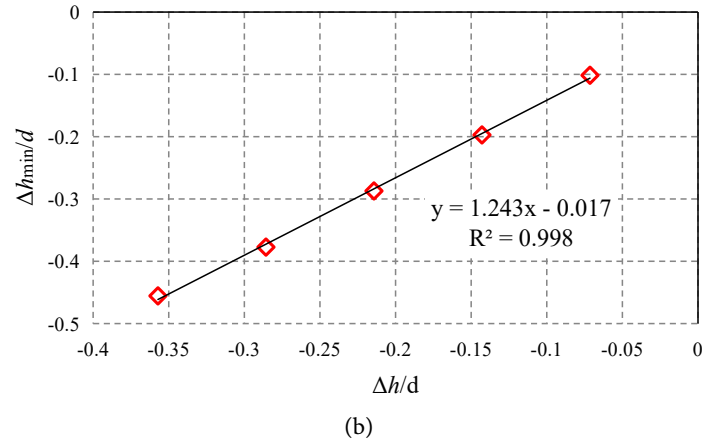


Figure 9. Variation of $\Delta h_{max}/d$ (a) and $\Delta h_{min}/d$ (b) with $\Delta h/d$.

Figure 10 respectively shows the variation of $\Delta h_{max}/d$ and $\Delta h_{min}/d$ with B/L . Under positive water level difference, with the increase of B/L , $\Delta h_{max}/d$ have obvious growth trend; while under negative water level difference, with the increase of B/L , $\Delta h_{min}/d$ first have a slight upward trend and then go to downward. In general, both of the variation is not large.

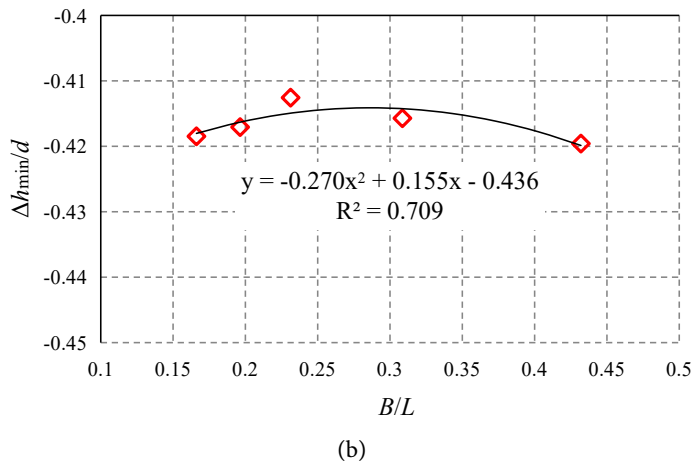
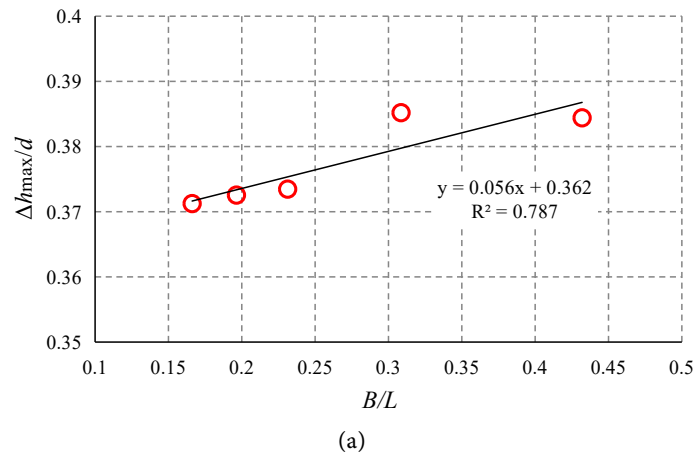
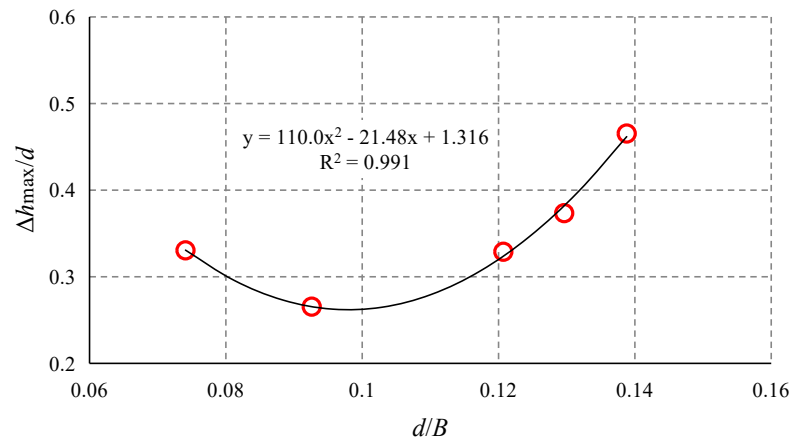
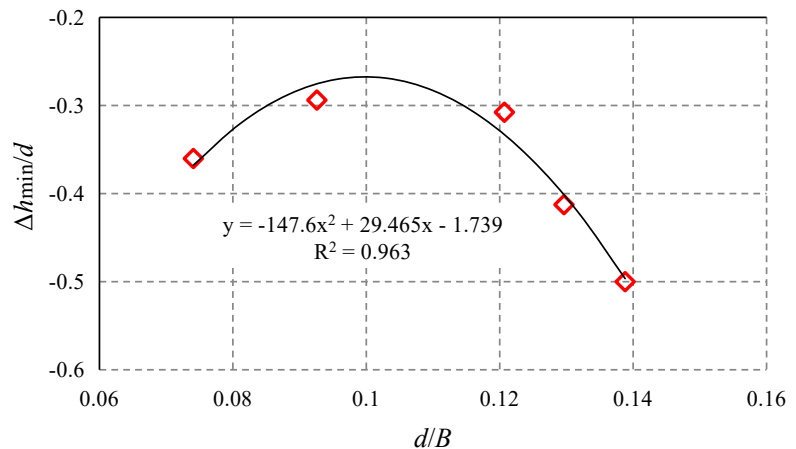


Figure 10. Variation of $\Delta h_{max}/d$ (a) and $\Delta h_{min}/d$ (b) with B/L .

Figure 11 respectively gives the variation of $\Delta h_{\max}/d$ and $\Delta h_{\min}/d$ with d/B . As indicated the relationship between $\Delta h_{\max}/d$ or $\Delta h_{\min}/d$ and d/B are both quadratic functions but with opposite opening directions. In terms of wave height absolute values, with increase of d/B , water fluctuation first increases and then decreases, which implies fluctuation is greater in narrow & deep or wide & shallow areas. Therefore, the proper design of chamber width and rational setting of water level in chamber can effectively reduce water fluctuation in chamber.



(a)



(b)

Figure 11. Variation of $\Delta h_{\max}/d$ (a) and $\Delta h_{\min}/d$ (b) with d/B .

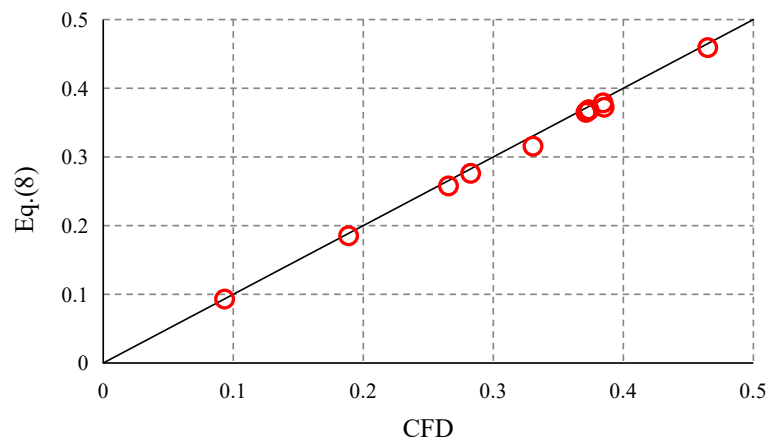
3.2. Empirical Formula

Through statistical analysis software SPSS, the results of **Figures 9-11** are regressed. And the empirical formula of $\Delta h_{\max}/d$ and $\Delta h_{\min}/d$ are fitted and expressed in Equation (8) and Equation (9). **Figure 12** shows the comparison of computed results between regression analysis and CFD. As described, the scatters are very close to the perfect line, which shows the fitting effect is satisfactory.

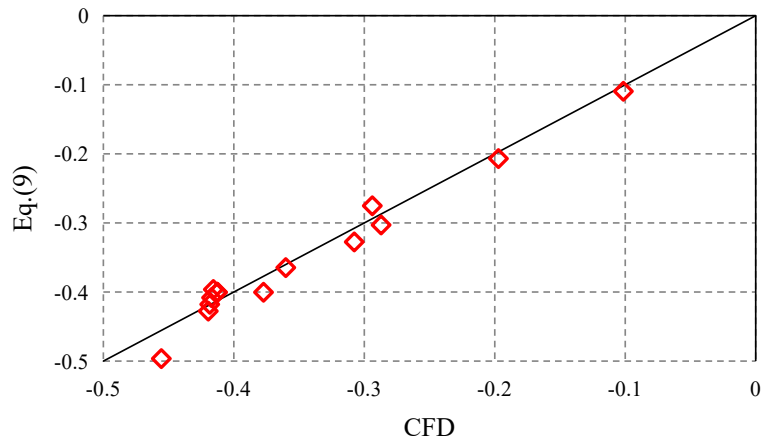
$$\frac{\Delta h_{\max}}{d} = 107.69 \left(\frac{d}{B} \right)^2 - 21.029 \frac{d}{B} + 0.052 \frac{B}{L} + 1.28 \frac{\Delta h}{d} + 0.904 \quad (8)$$

$$\frac{\Delta h_{\min}}{d} = -144.5 \left(\frac{d}{B}\right)^2 - 1.52 \left(\frac{B}{L}\right)^2 + 28.841 \frac{d}{B} + 0.872 \frac{B}{L} + 1.353 \frac{\Delta h}{d} - 1.441 \quad (9)$$

Due to the opening of actual tumble gate is a process and needs a certain time (labeled as t_v), building the relationship between computed results from simplified model and observed results from experimental model under different t_v can be a way to correct the simplified model results. **Figure 13** exhibits the variation of the difference (labeled as Δ) between observed and computed with different t_v under v_1 and v_2 . It is shown that the absolute values of observed wave height are always greater than computed either under positive difference or negative difference, which may be due to the actual opening way of tumble gate has a greater disturbance on water body. According to the fitting formulas in **Figure 13**, the correction formulas from simplified model to actual model are deduced, viz.



(a)



(b)

Figure 12. Comparison of the results between regression analysis and CFD.

$$\Delta h_{\max, \text{actual}} = \Delta h_{\max, \text{simplified}} - 0.119 t_v + 2.069 \quad (10)$$

$$\Delta h_{\min, \text{actual}} = \Delta h_{\min, \text{simplified}} - 0.036 t_v - 1.387 \quad (11)$$

Combining with the correction, the modified formulas of $\Delta h'_{\max}/d$ and $\Delta h'_{\min}/d$

are expressed in Equation (12) and Equation (13).

$$\frac{\Delta h'_{\max}}{d} = 107.69 \left(\frac{d}{B} \right)^2 - 21.029 \frac{d}{B} + 0.052 \frac{B}{L} + 1.28 \frac{\Delta h}{d} + 0.904 - \frac{0.119t_v}{d} + \frac{2.069}{d} \quad (12)$$

$$\frac{\Delta h'_{\min}}{d} = -144.5 \left(\frac{d}{B} \right)^2 - 1.52 \left(\frac{B}{L} \right)^2 + 28.841 \frac{d}{B} + 0.872 \frac{B}{L} + 1.353 \frac{\Delta h}{d} - 1.441 - \frac{0.036t_v}{d} - \frac{1.387}{d} \quad (13)$$

In Reference [6], considering the difficulty to modify the dimensions of chamber in experiments, only the chamber length L , chamber width B and tumble gate width D are unchanged, and the empirical formula obtained is also irrelevant to these variables. In this study, based on numerical simulation, we consider more variables, and the empirical formula is more applicable.

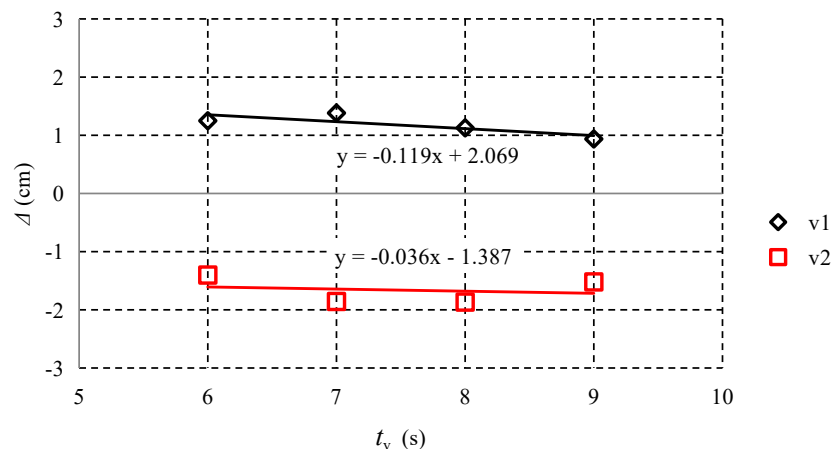


Figure 13. Variation of Δ as different t_v .

4. Discussion

In engineering practice, the flipping-opening of the gate of ship lift chamber is a dynamic process, involving the rotation of the gate, its interaction with the water, and the gradual change of the water flow. However, the simplified method of suddenly removing the gate in this paper ignores these dynamic details, resulting in an inability to accurately simulate the complex flow patterns in the initial stage of the water flow. The assumption of instantaneously removing the gate does not take into account the influence of the gate's presence on the flow boundary conditions. It overlooks the constraining and guiding effects of the gate structure on the water flow, rendering the simulation unable to fully represent the flow characteristics of the water under real boundary conditions. As indicated by Reference [11], when the opening speed of the gate of ship lift chamber is slow, the influence of the gate's opening time on the water surface fluctuation is negligible compared to the water level difference. Therefore, the empirical formula in the simplified

model of this paper is applicable to scenarios where the gate has a slow opening speed or a long opening time.

For more accurate simulation of the opening process of the ship lift chamber's gate, future research may consider adopting more complex models, such as the dynamic mesh technique based on Computational Fluid Dynamics (CFD), to precisely simulate the flipping motion of the gate and its interaction with the water flow. Meanwhile, the model can be calibrated and validated by combining experimental data so as to reduce errors. In addition, further exploration of simulation methods for multi-physics coupling is needed, taking into account factors such as water flow and structural mechanics comprehensively, so as to enhance the overall simulation capability of the hydraulic characteristics when opening and closing the gate of the ship lift chamber.

5. Conclusions

The simplified 3D numerical model of ship lift chamber upon tumble gate opening was built based on standard $k-\varepsilon$ model, finite volume method and VOF model. According to the numerical results, the following conclusions are summarized. The simplified mathematical model can obtain maximum and minimum wave height of the flow problem in this paper in general. Among the three influence factors, B/L has minimal impact on $\Delta h_{\max}/d$ or $\Delta h_{\min}/d$, while the influence of d/B and $\Delta h/d$ is relatively larger. The water level difference between chamber and approach channel, the water level in chamber and the chamber width have greater influence on the fluctuation of water surface in ship lift chamber. Therefore, trying to reduce water level difference, properly designing chamber width and reasonably setting water level in chamber can effectively reduce water fluctuation in chamber.

In the subsequent research, the focus will be on the hydraulic characteristics of the ship lift chamber during the actual opening and closing of the flip gate, which considers the opening and closing time of the flip gate and covers the situations with and without water level difference. It is further extended to the hydraulic analysis when there are ships moored in the ship lift chamber. Through in-depth research, a more accurate and scientific basis will be provided for the engineering design of the ship lift, and stronger technical support will be offered for the safety and stability of the ship lift during its operation, thus effectively ensuring the safe and efficient operation of the ship lift.

Acknowledgements

The contents of the paper were supported by Teacher Professional Development Program for Visiting Scholar (No. FX2021219), Scientific Research Fund of Zhejiang Provincial Education Department (No. Y202249386), and Zhejiang Provincial Teaching Reform Project (No. JGBA2024796).

Conflicts of Interest

The authors declare no conflicts of interest regarding the publication of this paper.

References

- [1] Hu, Y.A., Li, Z.H., Li, Y. and Xuan, G.X. (2016) Research Developments in the Field of Major Ship Lift in China. *Port & Waterway Engineering*, **12**, 10-19.
- [2] Tu, J., Qu, W. and Chen, J. (2008) An Experimental Study on Semi-Active Seismic Response Control of a Large-Span Building on Top of Ship Lift Towers. *Journal of Vibration and Control*, **14**, 1055-1074. <https://doi.org/10.1177/1077546307087396>
- [3] Wang, X., Hu, Y.A., Li, Z.H., *et al.* (2019) Prototype Monitoring of Mechanical Characteristics of Large Ship Lift Chamber Filling and Outletting of Water. *Hydro-Science and Engineering*, **3**, 1-8.
- [4] Hu, Y.A., Li, Z.H. and Lai, D.L. (2016) Influence of Different Tumble Gate Operation of Ship Lift Chamber on Vessels Mooring Force. *Port & Waterway Engineering*, **12**, 148-152.
- [5] Li, K., Mannan, M.A., Xu, M. and Xiao, Z. (2001) Electro-Hydraulic Proportional Control of Twin-Cylinder Hydraulic Elevators. *Control Engineering Practice*, **9**, 367-373. [https://doi.org/10.1016/s0967-0661\(01\)00003-x](https://doi.org/10.1016/s0967-0661(01)00003-x)
- [6] Gu, Z.H. (2000) Experimental Study on Hydrodynamic of Ship Lift Chamber. Master's Thesis, Nanjing Hydraulic Research Institute.
- [7] Wang, X. and Sun, Z.F. (2020) Influencing Factors of Ship Draught Control Standard Based on Prototype Test of Ship Lift. *Journal of Waterway and Harbor*, **41**, 578-584.
- [8] Fang, M. and Chen, T. (2008) A Parametric Study of Wave Loads on Trimaran Ships Traveling in Waves. *Ocean Engineering*, **35**, 749-762. <https://doi.org/10.1016/j.oceaneng.2008.02.001>
- [9] Gu, Z.H., Bao, G.J., Xuan, G.X. and Chen, J.Z. (2002) Experimental Study on Hydrodynamic Characteristics of Ship Lift Chambers. *Hydro Science and Engineering*, **3**, 7-13.
- [10] Gu, Z.H., Tang, H.W. and Li, Y. (2002) Computing Models of Maximum Longitudinal Hawser Force of Ship in Ship Lift Chamber. *Port & Waterway Engineering*, **1**, 10-13.
- [11] Gu, Z.H., Tang, H.W. and Li, Y. (2003) Neural Network Models of Maximum Fluctuation of Water Surface in Ship Lift Chamber with Tumble Gate Operating. *Journal of Yangtze River Scientific Research Institute*, **20**, 10-12.
- [12] Bao, G.J. and Chen, J.Z. (1998) Probe into Hydrodynamics Problems of Hoisting Vertical Ship Lift. *Hydro-Science and Engineering*, **4**, 397-403.
- [13] Yang, Z. (2015) Research of The Hydrodynamic Numerical Simulation Based on Ship Come in and out of the Vertical Ship Lift Chamber. Master's Thesis, Chongqing Jiaotong University.
- [14] Lynch, D.R. and Gray, W.G. (1980) Finite Element Simulation of Flow in Deforming Regions. *Journal of Computational Physics*, **36**, 135-153. [https://doi.org/10.1016/0021-9991\(80\)90180-1](https://doi.org/10.1016/0021-9991(80)90180-1)
- [15] Johns, B., Dube, S.K., Sinha, P.C., Mohanty, U.C. and Rao, A.D. (1982) The Simulation of a Continuously Deforming Lateral Boundary in Problems Involving the Shallow Water Equations. *Computers & Fluids*, **10**, 105-116. [https://doi.org/10.1016/0045-7930\(82\)90002-0](https://doi.org/10.1016/0045-7930(82)90002-0)
- [16] Primo, A.R.M., Wrobel, L.C. and Power, H. (2000) Boundary Integral Formulation for Slow Viscous Flow in a Deforming Region Containing a Solid Inclusion. *Engineering Analysis with Boundary Elements*, **24**, 53-63. [https://doi.org/10.1016/s0955-7997\(99\)00038-7](https://doi.org/10.1016/s0955-7997(99)00038-7)
- [17] Akyildiz, H. and Ünal, E. (2005) Experimental Investigation of Pressure Distribution

- on a Rectangular Tank Due to the Liquid Sloshing. *Ocean Engineering*, **32**, 1503-1516. <https://doi.org/10.1016/j.oceaneng.2004.11.006>
- [18] Akyildiz, H. and Erdem Ünal, N. (2006) Sloshing in a Three-Dimensional Rectangular Tank: Numerical Simulation and Experimental Validation. *Ocean Engineering*, **33**, 2135-2149. <https://doi.org/10.1016/j.oceaneng.2005.11.001>
- [19] Panigrahy, P.K., Saha, U.K. and Maity, D. (2009) Experimental Studies on Sloshing Behavior Due to Horizontal Movement of Liquids in Baffled Tanks. *Ocean Engineering*, **36**, 213-222. <https://doi.org/10.1016/j.oceaneng.2008.11.002>
- [20] Yeoh, S.L., Papadakis, G. and Yianneskis, M. (2004) Numerical Simulation of Turbulent Flow Characteristics in a Stirred Vessel Using the LES and RANS Approaches with the Sliding/Deforming Mesh Methodology. *Chemical Engineering Research and Design*, **82**, 834-848. <https://doi.org/10.1205/0263876041596751>
- [21] Dube, S.K., Sinha, P.C. and Roy, G.D. (1986) The Effect of a Continuously Deforming Coastline on the Numerical Simulation of Storm Surges in Bangladesh. *Mathematics and Computers in Simulation*, **28**, 41-56. [https://doi.org/10.1016/0378-4754\(86\)90086-8](https://doi.org/10.1016/0378-4754(86)90086-8)